QCD ⊕ QED NNLO corrections to Drell-Yan production

Daniel de Florian,* Manuel Der,† and Ignacio Fabre‡
International Center for Advanced Studies (ICAS), ECyT-UNSAM, Campus Miguelete, 25 de Mayo y Francia, 1650 Buenos Aires, Argentina

(Received 21 June 2018; published 12 November 2018)

We compute the QCD × QED [$\mathcal{O}(\alpha_s\alpha)$] mixed and QED^2 [$\mathcal{O}(\alpha^2)$] corrections to the production of an on-shell Z boson in hadronic collisions. We obtain them by profiting from the calculation of the pure QCD terms after taking the corresponding Abelian limits. Therefore, we extend the available knowledge up to complete next-to-next-to-leading-order precision in QCD ⊕ QED. We present explicit results for the perturbative coefficients and perform the phenomenological analysis at different collider energies with particular emphasis on the mixed corrections. We study the contribution from the different channels and discuss the scale dependence stabilization effect. We find that the contributions compete with the pure QCD NNLO ones under relevant kinematical conditions for the LHC, despite the fact that they are small, typically at the few per mille level.

DOI: 10.1103/PhysRevD.98.094008

I. INTRODUCTION

In recent years the development of high precision experiments in particle physics demanded a theoretical upgrade to match the accuracy achieved at the LHC. The state of the art in fixed order computations for processes with up to two hard partons in the final state is reaching next-to-next-to-leading order (NNLO), i.e., $\mathcal{O}(\alpha_s^2)$. Since $\alpha_s^2 \sim \alpha$, it becomes necessary to include also the corresponding next-to-leading-order (NLO) electroweak (EW) corrections, that for many observables exceed the few percent level (e.g., [1,2]) and become quantitatively important for an accurate description. Both precise measurements and calculations are essential to test different aspects of the Standard Model (SM) and to discern between them and possible new physics evidence due to beyond the Standard Model (BSM) effects.

In this sense, inclusive massive lepton pair production (the Drell-Yan process) has worked as an important test bed of perturbative quantum chromodynamics (QCD). On one hand, it has offered a sensitive way to study parton distribution functions (PDFs) [3–5]. From weak boson production, charge asymmetry measurements and invariant mass dependencies have helped to extract precise information on both the quarks' valence structure functions and the separation of quarks' flavors. On the other hand, knowing the behavior of charged-current (CC) and neutral-current (NC) processes has allowed us to perform high-precision measurements of fundamental electroweak parameters, like Z and W widths and masses and the EW mixing angle.

In addition, the Drell-Yan process is not only relevant to test SM predictions, but also to evaluate alternative BSM theories, where W and Z bosons usually appear as final or intermediate states in the decay of particles predicted in new physics models, like new gauge interactions, supersymmetry or heavy resonances [6].

In this sense, and considering that the improvement in statistics over the last years has made higher-order corrections experimentally noticeable, having access to QCD (and QED) corrections to these processes has become of great importance to put the previous predictions on a firmer ground.

Furthermore, recent work has been performed to include QED effects in the evolution of parton distributions, by providing explicit expressions for splitting kernels up to $\mathcal{O}(\alpha\alpha_s)$ [7] and $\mathcal{O}(\alpha^2)$ [8] and by the determination of precise photon distributions in the proton within the LUXqed approach [9,10], which are essential to match the theoretical calculations at the partonic level.

From the point of view of partonic cross sections, the $\mathcal{O}(\alpha)$ and $\mathcal{O}(\alpha\alpha_s)$ corrections represent the first EW and mixed-order contributions to Drell-Yan pair production in the general expansion

$$d\sigma = \sum_{i,j} \alpha_s^i \alpha^j d\sigma^{(i,j)}, \tag{1}$$

*deflo@unsam.edu.ar
†mder@unsam.edu.ar
‡ifabre@unsam.edu.ar

where pure EW $d\sigma^{(0,j)}$ and QCD $d\sigma^{(i,0)}$ corrections, as well as mixed-order contributions, which combine effects of the two interactions, arise.

So far, QCD corrections to the total cross section have been calculated at NLO in Ref. [11] and at NNLO in an inclusive way in Refs. [12–14]. Exclusive results have also been presented up to NNLO QCD accuracy [15–20]. Additionally, threshold calculations have been performed at next-to-next-to-next-to-leading-order (N^3LO) and next-to-next-to-next-to-leading-logarithmic (N^3LL) accuracy in Refs. [21,22].

On the other hand, concerning the EW contributions, exclusive computations for NLO-EW corrections to CC-DY are available in Refs. [23–25] and for NC-DY in Refs. [26,27]. Finally, progress towards the computation of NNLO-EW has been accomplished in recent years too [28–31]. Due to the lack of the full calculation of the NNLO mixed-order terms $\mathcal{O}(\alpha\alpha_s)$, different approaches have been followed to approximately combine the QCD and QED/EW corrections [32–36], by either assuming the full factorization or the additive combination of the strong and electroweak contributions. Particularly, recent partial exclusive results have been presented for the resonance region, by using the pole approximation [37–39].

The contributions for a general (i.e., including the decay of the gauge boson) perturbative calculation of Drell-Yan can be roughly characterized into purely factorizable terms that arise due to the initial state (production, from the initial state partons) and final state (decay, from the final state leptons) emissions and, on the other hand, nonfactorizable terms originated by soft photon exchange between the production and the decay. The nonfactorizable $\mathcal{O}(\alpha\alpha_s)$ contributions have been shown [37–39] to have a negligible impact on the cross section, allowing us to treat effectively Drell-Yan in the (resonant) limit of the decoupling between the production and decay processes, at least for the achieved experimental accuracy. The results presented in [39] also rely on the assumption that the missing initial-initial state factorizable $\mathcal{O}(\alpha\alpha_s)$ contributions are very small.

The computation of the so far unknown mixed QCD × QED $\mathcal{O}(\alpha\alpha_s)$ corrections to the inclusive on-shell production of a Z boson in hadronic collisions is the main goal of this paper. Those contributions are by themselves a gauge-invariant set of the complete Drell-Yan cross section calculation. Besides, QED corrections have been shown in [24,26] to be dominant over the pure weak ones at NLO, at least for distributions sensitive to recoil effects.[1] In this way, from now on we will make use of Eq. (1) in the sense of pure QED corrections instead of the full EW ones. Counting with analytical expressions for the total cross section can be useful to extend subtraction methods, such as q_T-subtraction [40] at $\mathcal{O}(\alpha\alpha_s)$.

In principle a full computation of QCD × QED $\mathcal{O}(\alpha\alpha_s)$ terms involves the evaluation of double-virtual, single-virtual plus one parton emission and double parton emission contributions, where a parton in general refers to quarks, antiquarks, gluons, and photons. Most of these double real contributions were recently presented in [41], including the case of W boson production which is not discussed in this paper,[2] while the master integrals for the two-loop calculation were obtained in [42].

Instead of following the path of a dedicated calculation for each term, in this work we profit from the available computation of NNLO pure QCD corrections $\mathcal{O}(\alpha_s^2)$ presented in [12] and, by pointing out the Abelian component, we extract the corresponding QCD × QED $\mathcal{O}(\alpha\alpha_s)$ contributions and assess the phenomenological impact for the inclusive cross section at different hadronic energies.

Furthermore, by following the same procedure we also present the QED^2 $\mathcal{O}(\alpha^2)$ corrections, completing, therefore, the set of NNLO contributions in QCD ⊕ QED [i.e., all terms that correspond to $i + j = 2$ in Eq. (1)].

This paper is organized as follows: In Sec. II we present the method used to compute the QCD × QED $\mathcal{O}(\alpha\alpha_s)$ and QED^2 $\mathcal{O}(\alpha^2)$ contributions from the pure QCD corrections $\mathcal{O}(\alpha_s^2)$. In Sec. III we present the results and study the detailed phenomenology of the corrections at different collider energies. Finally, in Sec. IV we present our conclusions. The explicit NNLO coefficients are presented in Appendix A.

II. ABELIANIZATION PROCEDURE

In order to achieve the $\mathcal{O}(\alpha\alpha_s)$ corrections we analyze the contributing diagrams for each channel in [12] and take the corresponding Abelian limit. To schematize this procedure, we describe the algorithm of gluon-photon interchange, taking as an example the most relevant $q\bar{q}$ channel.

For this explicit case, given that the color factors in the partonic cross section only depend on the QCD structure, without loss of generality we concentrate on diagrams with double real emission, which appear only to tree level. As can be observed in Fig. 1 there are four kinds of diagrams to consider, which we will label with the supraindex (k, l) according to the total number of QCD (k) and QED (l) vertices for each topology. Since the order of external momenta affects the color structure of the diagram, we will refer to the diagram shown in Fig. 1 as (a), while (a') represents the corresponding one obtained after crossing the final state parton lines.

[1] To take into account weak effects, one can work in the effective Born approximation, absorbing most of the pure weak contributions in an effective tree-level vectorial coupling between the Z boson and the quarks, so that only photonic corrections have to be considered and self-energy insertions in the Z (and eventually γ) propagator can be avoided [26].

[2] Only the contribution from the interference of QCD and QED $qq \to qq$ diagrams is missing in [41].

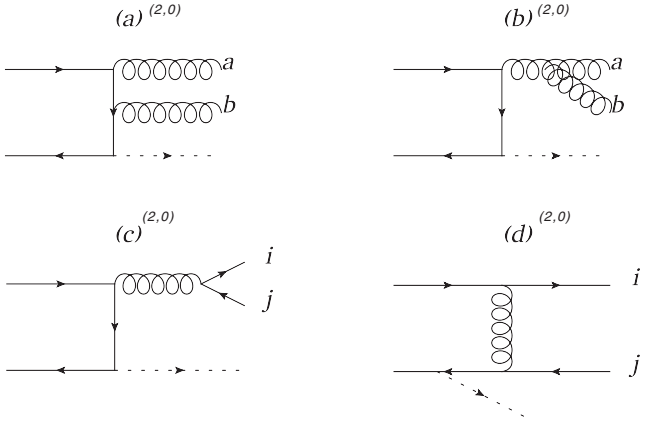

FIG. 1. Some of the diagrams contributing to NNLO QCD corrections to Drell-Yan.

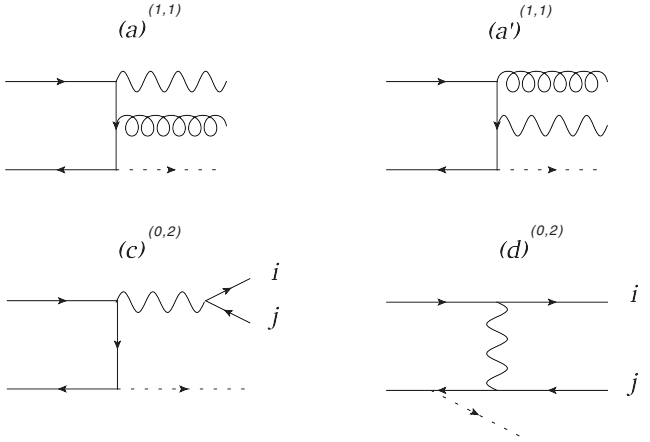

FIG. 2. Diagrams that result after applying the Abelianization procedure to the real NNLO QCD corrections in Fig. 1.

We can recognize different color factors, according to the configurations of color matrix traces in the calculation of each contribution to the partonic cross section. For example, terms corresponding to the calculation of $|(a)^{(2,0)}|^2$ in NNLO QCD turn out to be proportional to $\frac{1}{2N_C^2}\mathrm{Tr}[T^bT^aT^aT^b] = \frac{1}{2N_C}C_F^2$, where the N_C^2 in the denominator arises due to the average over the color factor of the incoming quarks and the symmetry factor $1/2$ is due to the appearance of two identical gluons in the final state. For the case of $[(a)^{(2,0)} \times (a'^*)^{(2,0)}]$ both Abelian and non-Abelian contributions appear, resulting in a factor $\frac{1}{2N_C^2}Tr[T^bT^aT^bT^a] = \frac{1}{2N_C}C_F(C_F - C_A/2)$ and, when considering terms from $[(b)^{(2,0)} \times (a^*)^{(2,0)}]$, they result proportional to $\frac{1}{2N_C^2}f^{abc}Tr[T^cT^aT^b] = -\frac{1}{2N_C}(C_FC_A/2)$, a purely non-Abelian contribution.

Once color factors are characterized for each term, we choose a gluon in the diagram, replace it by a photon and recalculate the color structure, thus obtaining modified diagrams with the corresponding new factors for QCD × QED corrections. These are shown in Fig. 2. Naturally, all the diagrams of type (b) vanish when considering the Abelian limit. Taking this into account, we find that the modified factors for $|(a)^{(1,1)}|^2$ and $[(a)^{(1,1)} \times (a'^*)^{(1,1)}]$ are both given by $\frac{e_q^2}{N_C^2}\mathrm{Tr}[T^aT^a] = \frac{e_q^2}{N_C}C_F$, where we have included the charge of the quark for the QED coupling. Here we may notice that all the color factors proportional to C_A, which corresponds to the non-Abelian part of the calculation, could be thrown out when considering the Abelian limit, while the ones proportional to C_F^2 are to be replaced by $2e_q^2C_F$, thus obtaining QCD × QED factors in each case.

It is worth noticing by performing the same analysis for the topology shown in Fig. 1(c), i.e., the production of a $q\bar{q}$ pair, that also the color factor T_R vanishes when the similar contribution is analyzed in the QCD × QED case, since the result for $[(c)^{(2,0)} \times (c^*)^{(0,2)}]$ becomes proportional to $\mathrm{Tr}[T^a]$. Therefore, since terms proportional to both C_A and T_R are vanishing, the same occurs for terms proportional to β_0^{QCD} in the original pure QCD calculation, consistent with the fact that no renormalization is needed at this order either for the QED or QCD couplings. Likewise, only a few contributions survive in the products of the type $[(c)^{(2,0)} \times (d^*)^{(0,2)}]$ and $[(d)^{(2,0)} \times (d'^*)^{(0,2)}]$, i.e., the interference of amplitudes with one photon and with one gluon exchange.

This strategy can be extended for all the topologies in $q\bar{q}$, and also for all channels, after treating carefully the initial color average factor.

In Table I we show the different color factors (after factorizing an overall factor of $1/2N_C$) for diagrams contributing to $\sigma^{(2,0)}$, and the resulting ones after the Abelianization procedure corresponding to $\sigma^{(1,1)}$. The replacements in the color structures needed to go from

TABLE I. Color factors corresponding to the $q\bar{q}$ channel for each contribution to NNLO QCD ⊕ QED corrections to Drell-Yan, up to an overall $\frac{1}{2N_C}$ factor. Focusing on α^2 factors, the third column includes sums over sets of quark (Q) and lepton (L) final state charges, while e_i and e_j refer to different quark flavor charges in the scattering.

Color factors in $q\bar{q}$			
Diagram	α_s^2	$\alpha \times \alpha_s$	α^2
$\lvert(a)\rvert^2$	C_F^2	$2e_q^2C_F$	e_q^4
$(d) \times (d^*)$	C_FT_R	0	$C_Ae_i^2e_j^2$
$(c) \times (c^*)$	$n_FC_FT_R$	0	$e_q^2[N_C\sum_{k\in Q}e_k^2 + \sum_{k\in L}e_k^2]$
$(a) \times (a'^*)$	$C_F^2 - \frac{C_FC_A}{2}$	$2e_q^2C_F$	e_q^4
$(d) \times (d'^*)$	$C_F^2 - \frac{C_FC_A}{2}$	$2e_q^2C_F$	e_q^4
$(b) \times (a^*)$	$-\frac{C_FC_A}{2}$	0	0
$(c) \times (d^*)$	$C_F^2 - \frac{C_FC_A}{2}$	$2e_q^2C_F$	e_q^4

the NNLO QCD coefficients to the QCD × QED ones can be directly read from the entries in Table I.

As an important feature, this method shows to be versatile in order to obtain NNLO QED corrections to Drell-Yan as well (i.e., the calculation of $\sigma^{(0,2)}$), if a deeper Abelian limit is considered. Here, by turning two gluons into photons from the topologies of NNLO QCD calculation one can recover correction terms up to second order in α, thus completing the set of QCD ⊕ QED NNLO corrections to Drell-Yan, in the sense of Eq. (1). The corresponding color factors for the $q\bar{q}$ channel (including electric charges of final state quarks and leptons) are also shown in Table I. The same occurs for other channels, after treating carefully the initial flux factor, which depends on the color properties of initial state particles. For instance, both $q\gamma$ and qg contributions to $\sigma^{(1,1)}$ can be obtained from the qg calculation for NNLO QCD corrections, by choosing the initial or final state gluon, respectively, to perform the Abelianization and following the procedure detailed above. Particularly, in the case of the γg channel, we have performed the explicit calculation of the fixed order corrections, finding perfect agreement with the result obtained by applying the Abelianization procedure.

III. RESULTS AND PHENOMENOLOGY

In general the cross section can be written as

$$\frac{d\sigma^Z}{dQ^2} = \tau\sigma(Q^2)W_Z(\tau, Q^2), \tag{2}$$

where $\sigma(Q^2)$ is the pointlike LO cross section; $\sqrt{S}$ is the hadronic center-of-mass energy; Q the invariant mass of the produced Z; $\tau = \frac{Q^2}{S}$; and $W_Z(\tau, Q^2)$ is the hadronic structure function.

The pointlike cross section that appears in Eq. (2) is defined as

$$\sigma(Q^2) = \frac{\sqrt{2}G_\mu M_Z}{4N_C}\frac{\Gamma_{Z\to X}}{(Q^2 - M_Z^2)^2 + M_Z^2\Gamma_Z^2}, \tag{3}$$

where $N_C = 3$ is the number of quark colors, $G_\mu = 1.1663910^{-5}$ GeV^{-2} is the *muon* Fermi constant, $M_Z = 91.187$ GeV and Γ_Z are the mass and width of the Z, and $\Gamma_{Z\to X}$ is the partial width due to the decay of the Z to X (e.g., for leptonic decay, $X = \ell\bar{\ell}$).[3] The narrow-width approximation used in this paper consists of making the following replacement:

$$\frac{1}{(Q^2 - M_Z^2)^2 + M_Z^2\Gamma_Z^2} \to \frac{\pi}{M_Z\Gamma_Z}\delta(Q^2 - M_Z^2), \tag{4}$$

[3]Note that although other EW parameter schemes can been used, at this order of perturbation theory the discrepancies may be numerically significant.

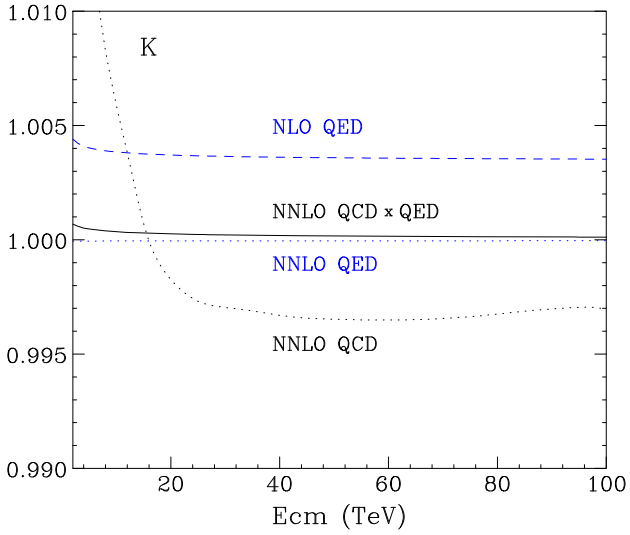

FIG. 3. K-factors for the different distributions as defined in Eq. (6). The (blue) dashed line corresponds to $K_{\rm QED}^{\rm NLO}$, the (blue) dotted line to $K_{\rm QED}^{\rm NNLO}$, the solid line to the mixed $K_{\rm QCD\times QED}^{\rm NNLO}$ and the (black) dotted line to the pure NNLO QCD corrections $K_{\rm QCD}^{\rm NNLO}$.

ensuring the decoupling of the production and decay mechanisms. The hadronic structure function appearing in (2) can be written as a sum of contributions of different orders:

$$W_Z(\tau, Q^2) = \int_0^1 dx_1 \int_0^1 dx_2 \int_0^1 dx \delta(\tau - x x_1 x_2) \times \sum_{i,j}\left(\frac{\alpha_s}{4\pi}\right)^i \left(\frac{\alpha}{4\pi}\right)^j w_Z^{(i,j)}(x, x_1, x_2, Q^2), \tag{5}$$

where the dependence on the factorization μ_F and renormalization μ_R scales is implicit.

The analytic expressions for the inclusive cross section of Drell-Yan Z-production at QCD ⊕ QED NNLO are presented in Appendix A.

To study the phenomenology of the total inclusive cross section, i.e., in all the decay channels of the Z within the narrow-width approximation, a specific code was written which makes use of the LHAPDF [43] package to interpolate sets of parton distribution functions. Unless explicitly stated, we set the renormalization and factorization scales to $\mu_R = \mu_F = M_Z$. For both interactions, we set the running coupling at the corresponding renormalization scale [i.e., $\alpha(M_Z) \sim \frac{1}{128}$] and always use the parton distributions to NNLO (QCD) accuracy [3–5,44] with the corresponding QED corrections from the set LUXqed17_plus_PDF4LHC15_nnlo_100 [9,10].[4] In Fig. 3 we plot the

[4]It should be noted that this set includes splitting functions of order $\mathcal{O}(\alpha_s\alpha)$ and $\mathcal{O}(\alpha^2)$. For the results presented in this work, one order further would be needed to perform a fully consistent evolution of the PDFs.

K-factors for different orders as a way to quantify the size of the QED and QCD corrections to Drell-Yan at different center-of-mass energies.

Here the K-factor is defined as the ratio of the cross section computed at a given order over the previous one, i.e.,

$$K_{\rm QED}^{\rm NLO} = \frac{\sigma^{(0,0)} + \alpha\sigma^{(0,1)}}{\sigma^{(0,0)}}$$
$$K_{\rm QCD}^{\rm NNLO} = \frac{\sigma^{(0,0)} + \alpha_s\sigma^{(1,0)} + \alpha_s^2\sigma^{(2,0)}}{\sigma^{(0,0)} + \alpha_s\sigma^{(1,0)}}$$
$$K_{\rm QED}^{\rm NNLO} = \frac{\sigma^{(0,0)} + \alpha\sigma^{(0,1)} + \alpha^2\sigma^{(0,2)}}{\sigma^{(0,0)} + \alpha\sigma^{(0,1)}}$$
$$K_{\rm QCD\times QED}^{\rm NNLO} = \frac{\sigma^{(0,0)} + \alpha\sigma^{(0,1)} + \alpha_s\sigma^{(1,0)} + \alpha\alpha_s\sigma^{(1,1)}}{\sigma^{(0,0)} + \alpha\sigma^{(0,1)} + \alpha_s\sigma^{(1,0)}}. \quad (6)$$

As can be observed, the NNLO QCD corrections are of the same (∼5 per mille level) order, but typically with the opposite sign, as the NLO QED corrections, as expected from the simple counting $\alpha_s^2 \sim \alpha$. The mixed QCD × QED turn out to be positive and below the per mille level over the whole range of energies spanned in the plot. Interestingly, due to the particular dependence of the NNLO QCD corrections with the energy, with a sign change around $\sqrt{S} \sim 16$ TeV, for the LHC at $\sqrt{S} \sim 14$ TeV the mixed QCD × QED corrections are only a factor of ∼3.5 smaller than the pure NNLO QCD contributions. Furthermore, for lower center-of-mass energies $\sqrt{S} \sim 2$ TeV the mixed terms almost reach the per mille level and are just a factor of 5 smaller than the NLO QED ones, showing that the elementary counting of couplings can fail under certain kinematical conditions. The pure NNLO QED terms, also plotted in Fig. 3, are negative but the corrections always remain at the $\mathcal{O}(10^{-5})$ level.

Even though for this particular observable the mixed QCD × QED contributions are small, it is interesting to study how well they can be approximated by the factorization assumption on QED plus QCD corrections, where it is assumed that $\kappa_{\rm fact} = [K_{\rm QED}^{\rm NLO} \times K_{\rm QCD}^{\rm NLO}]_{\mathcal{O}(\alpha\alpha_s)} = \alpha\alpha_s \frac{\sigma^{(0,1)}\sigma^{(1,0)}}{\sigma^{(0,0)}\sigma^{(0,0)}}$, compared to the exact case $\kappa_{\rm mixed} = \alpha\alpha_s \frac{\sigma^{(1,1)}}{\sigma^{(0,0)}}$. For that purpose, we define the following quantity:

$$R = \frac{\kappa_{\rm mixed}}{\kappa_{\rm fact}} = \frac{\sigma^{(0,0)}\sigma^{(1,1)}}{\sigma^{(0,1)}\sigma^{(1,0)}}, \quad (7)$$

which is the ratio between the exact and the approximated factorized contribution. Although this approximation is well motivated in many cases, in this particular process there is no reason to expect it to work. In fact, as it can be observed in Fig. 4, the factorization approach fails to reproduce the correct behavior of the mixed contribution typically by a factor of 2 or more. Of course, given the size of the corrections, the effect of the factorized treatment of these contributions is small at the level of the cross section, as shown in the inset plot of Fig. 4, where we show the ratio between the cross section computed exactly and within the factorization approach, but the situation might not hold for other observables or even for more exclusive distributions in Drell-Yan.

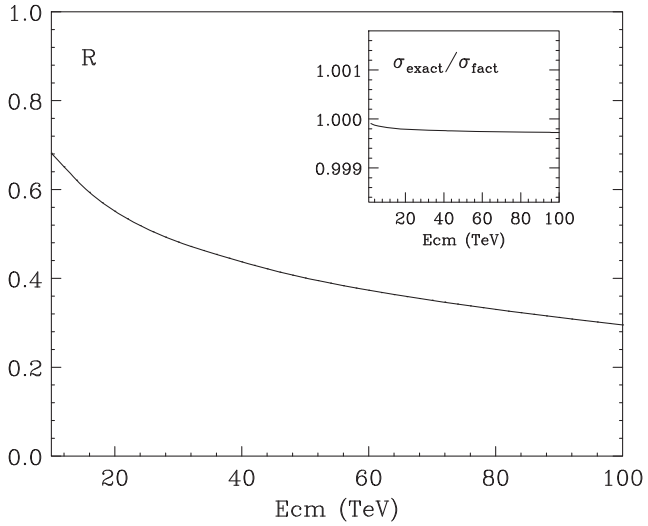

FIG. 4. Ratio R between the exact and the factorization approximation for the mixed QCD × QED contributions. The inset plot shows the ratio of the cross section computed exactly and with the factorization approximation for the mixed term.

In Fig. 5 we show the contribution to the mixed QCD × QED K-factor from the different channels. It is noticeable that the photon initiated contributions are rather small, mostly due to the size of the photon PDF in the proton, as can be observed by comparing $q\gamma$ and qg contributions, which share the same partonic coefficient apart from the color factor. It is also clear that the different signs of qq (fully dominated by the Born level $q\bar{q}$ channel and exceeding the per mille level) and qg contributions conspire to

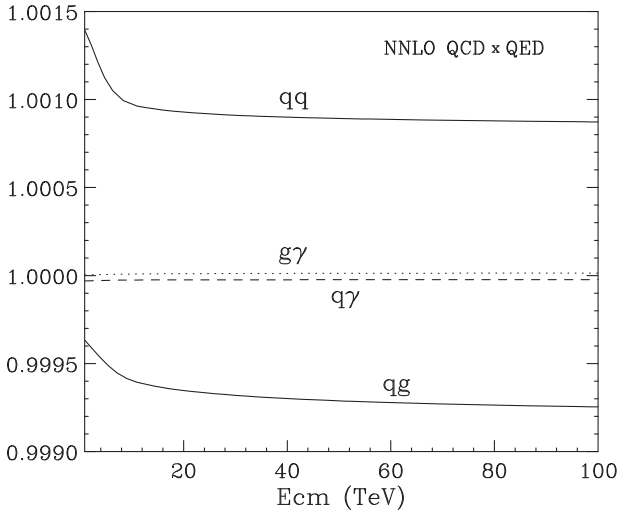

FIG. 5. Contribution to the mixed QCD × QED K-factor from the different channels. Here the label q accounts for both quarks and antiquarks and qq represents the sum of $q\bar{q}$ and qq.

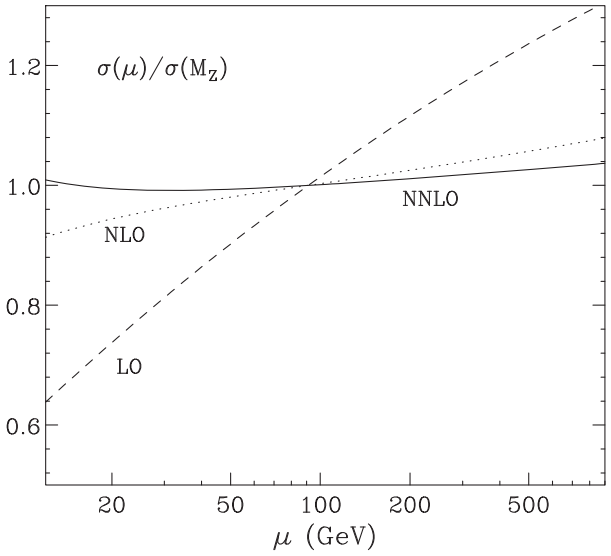

FIG. 6. Cross sections corresponding to LO [dashes, $i+j=0$ in Eq. (1)], NLO (dots, $i+j=0,1$) and NNLO (solid, $i+j=0,1,2$) at different factorization and renormalization scales with $\mu_R=\mu_F=\mu$. All results are normalized by the corresponding cross section at $\mu=M_Z$.

reduce the effect of the mixed QCD × QED corrections to the Drell-Yan cross section. Again, in more exclusive distributions this partial cancellation might be spoiled by some kinematical cuts, resulting in an increase of the mixed-order corrections.

Finally, we discuss the effect of the higher order contributions in the stabilization of the perturbative expansion in terms of the scale dependence for $\sqrt{S}=13$ TeV (very similar behaviors are observed for other values of $\sqrt{S}$). In Fig. 6 we show the LO ($\sigma^{(0,0)}$), NLO ($\sigma^{(0,0)}+\alpha\sigma^{(0,1)}+\alpha_s\sigma^{(1,0)}$) and NNLO ($\sigma^{(0,0)}+\alpha\sigma^{(0,1)}+\alpha_s\sigma^{(1,0)}+\alpha\alpha_s\sigma^{(1,1)}+\alpha^2\sigma^{(0,2)}+\alpha_s^2\sigma^{(2,0)}$) cross sections for different values of the factorization and renormalization scales $\mu_R=\mu_F=\mu$, normalized by the corresponding value at the central scale $\mu=M_Z$. From the slope of the different curves, it is clearly visible the reduction in the scale dependence when including higher order corrections, mostly due to the dominant QCD effects. At NLO the QED corrections contribute less than 1%, increasing the scale dependence introduced by QCD corrections. At NNLO, the inclusion of the mixed-order terms as well as pure QED corrections (that make up less than 0.1% of the total cross section) reduce the scale dependence introduced by pure QCD corrections.

IV. CONCLUSIONS

In conclusion, mixed QCD × QED as well as pure QED^2 NNLO corrections to the total Drell-Yan Z-production cross section were presented for the first time. This was achieved via an Abelianization procedure that profits from the available pure QCD NNLO result and proved to be a versatile technique. We performed the phenomenological analysis finding that the mixed corrections are of the order of per mille at the LHC, but only a factor of ∼3.5 smaller than the pure QCD NNLO due to a sign change that occurs in the latter at $\sqrt{S}\sim 16$ TeV. Pure QED NNLO terms are shown to be negative corrections of the order of 10^{-5}. The full QCD ⊕ QED NNLO corrections are found to further stabilize the scale dependence of the final result. The exact K-factor at order $\mathcal{O}(\alpha\alpha_s)$ was compared with the naive factorization approximation, which consists of the mixed-order term of the product of QCD and QED NLO K-factors. It was shown that the latter fails to reproduce the exact result by a factor of 2 or more. Although in this case the difference is not significant, due to the smallness of the overall contribution, this result hints that the factorization approximation may not work for other processes nor for more exclusive measurements of the one presented herein.

ACKNOWLEDGMENTS

The work of D. de F. has been partially supported by Conicet, ANPCyT and the von Humboldt Foundation. We thank Massimiliano Grazzini, Leandro Cieri, German Sborlini and Javier Mazzitelli for discussions and comments on the manuscript.

APPENDIX A: DEFINITIONS AND NOTATION

Here we present for the first time the coefficients $w_Z^{(1,1)}$ and $w_Z^{(0,2)}$ in the sense of Eq. (5). They include the NNLO mixed QED × QCD and QED corrections, respectively:

$$\begin{aligned} w_Z^{(1,1)} &= \sum_{i\in Q,\bar{Q}} q_i(x_1)\bar{q}_i(x_2)c_i 2e_i^2 C_F \Delta_{q\bar{q}}^{(2)C_F}(x) + \sum_{i\in Q,\bar{Q}} q_i(x_1)q_i(x_2)c_i 2e_i^2 C_F \Delta_{qq}^{(2)\mathrm{id}}(x) \\ &+ \sum_{i\in Q,\bar{Q}} [2C_A C_F(q_i(x_1)\gamma(x_2)+\gamma(x_1)q_i(x_2)) + (q_i(x_1)g(x_2)+g(x_1)q_i(x_2))]c_i e_i^2 \Delta_{qg}^{(2)C_F}(x) \\ &+ (g(x_1)\gamma(x_2)+\gamma(x_1)g(x_2))2C_A\left(\sum_{k\in Q} c_k e_k^2\right)\Delta_{gg}^{(2)}(x) \end{aligned} \tag{A1}$$

$$
\begin{aligned}
w_Z^{(0,2)} = & \sum_{i\in Q,\bar{Q}} q_i(x_1)\bar{q}_i(x_2)\Bigg\{ c_i e_i^2 \left(e_i^2 \Delta_{q\bar{q}}^{(2)C_F}(x) + 2\left[N_C \sum_{k\in Q} e_k^2 + \sum_{k\in L} e_k^2 \right] \Delta_{q\bar{q}}^{(2)n_F}(x) + \beta_0^{\mathrm{QED}} \Delta_{q\bar{q}}^{(1)}(x) \log\left(\frac{\mu_R^2}{\mu_F^2}\right) \right) \\
& + \sum_{k\in Q} [c_k \Delta_{q\bar{q}}^{(2)f}(x) + a_i a_k \Delta_{q\bar{q}}^{(2)ax}(x)] 2C_A e_i^2 e_k^2 + \sum_{k\in L} [c_k \Delta_{q\bar{q}}^{(2)f}(x) + a_i a_k \Delta_{q\bar{q}}^{(2)ax}(x)] 2 e_i^2 e_k^2 \Bigg\} \\
& + \sum_{i\in Q,\bar{Q}} c_i q_i(x_1) q_i(x_2) \Delta_{qq}^{(2)\mathrm{id}}(x) e_i^4 + \sum_{i,j\in Q,\bar{Q}} q_i(x_1) q_j(x_2) 2C_A e_i^2 e_j^2 \\
& \times [(c_i + c_j)\Delta_{qq}^{(2)\mathrm{non\text{-}id}}(x) + v_i v_j \Delta_{q_i q_j}^{(2)\mathrm{non\text{-}id,V}}(x) + a_i a_j \Delta_{qq}^{(2)\mathrm{non\text{-}id,A}}(x)] \\
& + \sum_{i\in Q,\bar{Q}} (q_i(x_1)\gamma(x_2) + \gamma(x_1) q_i(x_2)) c_i 2C_A e_i^2 \left[e_i^2 \Delta_{qg}^{(2)C_F}(x) + \beta_0^{\mathrm{QED}} \Delta_{qg}^{(1)\gamma}(x) \log\left(\frac{\mu_R^2}{\mu_F^2}\right) \right] \\
& + \gamma(x_1)\gamma(x_2) 4C_A \left[N_C \sum_{k\in Q} c_k e_k^4 + \sum_{k\in L} c_k e_k^4 \right] \Delta_{gg}^{(2)C_F}(x),
\end{aligned} \tag{A2}
$$

where $Q(\bar{Q})$ and L are the sets of (anti)quarks and leptons considered (e.g., $Q = \{u, d, c, s, b\}$, $L = \{e, \mu, \tau\}$), e_k is the charge of the particle k in units of the electron charge, μ_F and μ_R are the factorization and renormalization scales, $c_i = v_i^2 + a_i^2$ with v_i and a_i defined as the vector and axial couplings of particle i:

$$v_u = 1 - \frac{8}{3}\sin^2\theta_W, \qquad a_u = -1, \tag{A3}$$

$$v_d = -1 + \frac{4}{3}\sin^2\theta_W, \qquad a_d = 1, \tag{A4}$$

$$v_e = -1 + 4\sin^2\theta_W, \qquad a_e = 1, \tag{A5}$$

and replicated through families, the QED and QCD beta functions are given by

$$
\begin{aligned}
\beta_0^{\mathrm{QED}} &= -\frac{2}{3}\left(N_C \sum_{k\in Q} e_k^2 + \sum_{k\in L} e_k^2 \right) \\
\beta_0^{\mathrm{QCD}} &= \frac{11}{3} C_A - \frac{2}{3} n_F,
\end{aligned} \tag{A6}
$$

n_F is the number of quark flavors considered ($n_F = \#Q$), and the various $\Delta(x)$ correction functions are defined in Appendix B.

The other coefficients needed for the full NNLO calculation, $w_Z^{(i,0)}$ for $i \le 2$ and $w^{(0,1)}$, were presented in [12] and [26,27] respectively. Here they are rewritten in this notation for the sake of completeness and as a reference for the full set of NNLO corrections to the Drell-Yan Z production:

$$w_Z^{(0,0)} = \sum_{i\in Q,\bar{Q}} c_i q_i(x_1)\bar{q}_i(x_2)\delta(1-x) \tag{A7}$$

$$w_Z^{(1,0)} = \sum_{i\in Q,\bar{Q}} \{c_i q_i(x_1)\bar{q}_i(x_2) C_F \Delta_{q\bar{q}}^{(1)}(x)(q_i(x_1) g(x_2) + g(x_1) q_i(x_2)) c_i \Delta_{qg}^{(1)}(x)\} \tag{A8}$$

$$w_Z^{(0,1)} = \sum_{i\in Q,\bar{Q}} \{c_i q_i(x_1)\bar{q}_i(x_2) e_i^2 \Delta_{q\bar{q}}^{(1)}(x)(q_i(x_1)\gamma(x_2) + \gamma(x_1) q_i(x_2)) c_i 2C_A e_i^2 \Delta_{qg}^{(1)}(x)\} \tag{A9}$$

$$
\begin{aligned}
w_Z^{(2,0)} = & \sum_{i\in Q,\bar{Q}} q_i(x_1)\bar{q}_i(x_2)\Bigg\{ c_i C_F \left(C_A \Delta_{q\bar{q}}^{(2)C_A}(x) + C_F \Delta_{q\bar{q}}^{(2)C_F}(x) + n_F \Delta_{q\bar{q}}^{(2)n_F}(x) + \beta_0^{\mathrm{QCD}} \Delta_{q\bar{q}}^{(1)}(x) \log\left(\frac{\mu_R^2}{\mu_F^2}\right) \right) \\
& + \sum_{k\in Q} [c_k \Delta_{q\bar{q}}^{(2)f}(x) + a_i a_k \Delta_{q\bar{q}}^{(2)ax}(x)] C_F \Bigg\} + \sum_{i\in Q,\bar{Q}} c_i q_i(x_1) q_i(x_2) \Delta_{qq}^{(2)\mathrm{id}}(x) C_F \left(C_F - \frac{1}{2} C_A \right) \\
& + \sum_{i,j\in Q,\bar{Q}} q_i(x_1) q_j(x_2) C_F [(c_i + c_j)\Delta_{qq}^{(2)\mathrm{non\text{-}id}}(x) + v_i v_j \Delta_{q_i q_j}^{(2)\mathrm{non\text{-}id,V}}(x) + a_i a_j \Delta_{qq}^{(2)\mathrm{non\text{-}id,A}}(x)] \\
& + \sum_{i\in Q,\bar{Q}} (q_i(x_1) g(x_2) + g(x_1) q_i(x_2)) c_i \left[C_A \Delta_{qg}^{(2)C_A}(x) + C_F \Delta_{qg}^{(2)C_F}(x) + \beta_0^{\mathrm{QCD}} \Delta_{qg}^{(1)}(x) \log\left(\frac{\mu_R^2}{\mu_F^2}\right) \right] \\
& + g(x_1) g(x_2) \left(\sum_{k\in Q} c_k \right) (\Delta_{gg}^{(2)C_A}(x) + \Delta_{gg}^{(2)C_F}(x)).
\end{aligned} \tag{A10}
$$

APPENDIX B: ANALYTIC EXPRESSIONS FOR CORRECTION TERMS

In order to present the expressions for the different corrections, we define the following distributions:

$$\mathcal{D}_i(x) = \left[\frac{\ln^i(1-x)}{1-x}\right]_+ \tag{B1}$$

which appear in the soft terms regularizing the divergence of soft emission ($x \approx 1$) and defined as usual by

$$\int_0^1 \mathcal{D}_i(x) f(x) \mathrm{d}x = \int_0^1 \frac{\ln^i(1-x)}{1-x}[f(x) - f(1)]\mathrm{d}x. \tag{B2}$$

We also define an auxiliary variable to write the dependence on the factorization scale,

$$L_{\mu_F} = \ln\left(\frac{\mu_F^2}{Q^2}\right), \tag{B3}$$

where μ_F is the factorization scale and Q the invariant mass of the produced Z.

The corrections needed for the NLO result are

$$\Delta_{q\bar{q}}^{(1)} = 8\mathcal{D}_0(x)L_{\mu_F} + 16\mathcal{D}_1(x) + \delta(x-1)(6L_{\mu_F} + 8\zeta_2 - 16) - 4L_{\mu_F}(x+1) - \frac{4(x^2+1)\ln(x)}{1-x} - 8(x+1)\ln(1-x) \tag{B4}$$

$$\Delta_{qg}^{(1)} = \frac{1}{2}(2(2x^2 - 2x + 1)(L_{\mu_F} + 2\ln(1-x) - \ln(x)) - 7x^2 + 6x + 1). \tag{B5}$$

For the second NNLO, several correction terms are introduced. We denote with a C_A superscript the corrections coming from the non-Abelian part of the contributions (only relevant for the QCD NNLO contribution), with n_F the ones that involve a sum over fermion families (relevant for the QCD and QED NNLO result), and with C_F the rest of the Abelian contributions.

The non-Abelian contributions on the quark-antiquark channel are

$$\Delta_{q\bar{q}}^{(2)C_A} = \Delta_{q\bar{q}}^{\mathrm{NS},C_A} - \Delta_{q\bar{q}}^{C_F - C_A/2} \tag{B6}$$

$$\Delta_{q\bar{q}}^{(2)C_F} = \Delta_{q\bar{q}}^{\mathrm{NS},C_F} + 2\Delta_{q\bar{q}}^{C_F - C_A/2} \tag{B7}$$

$$\begin{aligned}
\Delta_{q\bar{q}}^{(2)n_F} = {} & \frac{8}{27}(9\mathcal{D}_0(x)L_{\mu_F}^2 + L_{\mu_F}(36\mathcal{D}_1(x) - 30\mathcal{D}_0(x)) - 36\mathcal{D}_0(x)\zeta_2 + 28\mathcal{D}_0(x) \\
& - 60\mathcal{D}_1(x) + 36\mathcal{D}_2(x)) + \frac{1}{18}\delta(x-1)(36L_{\mu_F}^2 - 204L_{\mu_F} - 224\zeta_2 + 144\zeta_3 + 381) \\
& + \frac{1}{27(x-1)}(2(2(18x^2\mathrm{Li}_2(1-x) - (x-1)(9L_{\mu_F}^2(x+1) + L_{\mu_F}(6 - 66x) \\
& - 36x\zeta_2 + 103x - 36\zeta_2 - 47)) - 24\ln(1-x)((x-1)(3L_{\mu_F}(x+1) - 11x + 1) \\
& - 6(x^2+1)\ln(x)) + 18(4L_{\mu_F}(x^2+1) - 11x^2 + 10x - 9)\ln(x) - 72(x^2-1)\ln^2(1-x) \\
& - 9(5x^2+7)\ln^2(x))),
\end{aligned} \tag{B8}$$

where we amended the result for $\Delta_{q\bar{q},A^2}^{(2)}$ given in Eq. (B.11) of Ref. [12] by adding the corresponding missing x factor to term $103x$ above, and where

$$\Delta_{q\bar{q}}^{\mathrm{NS},C_A} = \frac{1}{180}\delta(x-1)(-1980L_{\mu_F}^2 - 4320L_{\mu_F}\zeta_3 + 11580L_{\mu_F} - 432\zeta_2^2 + 11840\zeta_2 + 5040\zeta_3 - 23025) - \frac{4}{27}(99\mathcal{D}_0(x)L_{\mu_F}^2 + 108\mathcal{D}_0(x)L_{\mu_F}\zeta_2 - 402\mathcal{D}_0(x)L_{\mu_F} - 396\mathcal{D}_0(x)\zeta_2 - 378\mathcal{D}_0(x)\zeta_3 + 404\mathcal{D}_0(x) + 396\mathcal{D}_1(x)L_{\mu_F} + 216\mathcal{D}_1(x)\zeta_2 - 804\mathcal{D}_1(x) + 396\mathcal{D}_2(x)) + \frac{1}{27(x-1)}[2(36\mathrm{Li}_2(1-x)(3L_{\mu_F}(x^2+1) - 7x^2 + 3x + 3) + 99L_{\mu_F}^2(x^2-1) + 6L_{\mu_F}(x-1)(2x(9\zeta_2 - 62) + 18\zeta_2 - 19) + 270x^2\mathrm{S}_{1,2}(1-x) - 162\mathrm{S}_{1,2}(1-x) + 324\mathrm{Li}_3(1-x) - 450x^2\zeta_2 - 378x^2\zeta_3 + 1139x^2 + 108x\zeta_2 - 1362x + 342\zeta_2 + 378\zeta_3 + 223) + 12\ln(1-x) \times (36x^2\mathrm{Li}_2(1-x) + (x-1)(66L_{\mu_F}(x+1) + 36x\zeta_2 - 239x + 36\zeta_2 - 38) - 6(22x^2+13)\ln(x)) - 18\ln(x)(12(x^2+1)\mathrm{Li}_2(1-x) + L_{\mu_F}(44x^2+26) + 12x^2\zeta_2 - 109x^2 + 83x + 12\zeta_2 - 78) + 792(x^2-1)\ln^2(1-x) + 9(55x^2+32)\ln^2(x)] \tag{B9}$$

$$\Delta_{q\bar{q}}^{\mathrm{NS},C_F} = L_{\mu_F}(-\mathcal{D}_0(x)(64\zeta_2 + 128) + 96\mathcal{D}_1(x) + 192\mathcal{D}_2(x)) + L_{\mu_F}^2(48\mathcal{D}_0(x) + 64\mathcal{D}_1(x)) + 256\mathcal{D}_0(x)\zeta_3 - \mathcal{D}_1(x)(128\zeta_2 + 256) + 128\mathcal{D}_3(x) + \delta(x-1) \times \left(L_{\mu_F}^2(18 - 32\zeta_2) + L_{\mu_F}(24\zeta_2 + 176\zeta_3 - 93) + \frac{8\zeta_2^2}{5} - 70\zeta_2 - 60\zeta_3 + \frac{511}{4}\right) + \frac{1}{3(x-1)}[2(12(\mathrm{Li}_2(1-x)(2L_{\mu_F}(x^2-3) - 4x^2 + x + 3) + L_{\mu_F}^2(-(x^2+4x-5)) + L_{\mu_F}(x-1)(x(4\zeta_2+2) + 4\zeta_2 + 15) + 6x^2\mathrm{S}_{1,2}(1-x) + 2\mathrm{S}_{1,2}(1-x) - 4x^2\mathrm{Li}_3(1-x) + 6\mathrm{Li}_3(1-x) - 8x^2\zeta_2 - 16x^2\zeta_3 + 6x^2 + 16x\zeta_2 - 15x - 8\zeta_2 + 16\zeta_3 + 9) + 6\ln(1-x) \times (6(x^2-3)\mathrm{Li}_2(1-x) - (x-1)(8L_{\mu_F}^2(x+1) - 4L_{\mu_F}(x-7) - x(16\zeta_2+3) - 16(\zeta_2+4)) + 4(L_{\mu_F}(9x^2+5) - 7x^2 + 11x - 4)\ln(x) - 12(2x^2+1)\ln^2(x)) + 12\ln(x)(3(x^2+1)\mathrm{Li}_2(1-x) + L_{\mu_F}^2(3x^2+1) + L_{\mu_F}(-3x^2 + 10x - 1) - 12x^2\zeta_2 + 6x^2 - 19x - 4\zeta_2 - 1) - 6\ln^2(1-x)(8(x-1)(3L_{\mu_F}(x+1) - 2x + 2) - (39x^2+23)\ln(x)) - 6(L_{\mu_F}(9x^2+3) - 6x^2 + 8x - 2)\ln^2(x) - 96(x^2-1)\ln^3(1-x) + (25x^2+11)\ln^3(x))] \tag{B10}$$

$$\Delta_{q\bar{q}}^{C_F - C_A/2} = \frac{1}{3(x-1)}(12\mathrm{Li}_2(1-x)(2L_{\mu_F}x^2 + 2L_{\mu_F} - 9x^3 + 4x^2 + 4(x^2+1)\ln(1-x) + 2(2x^3 + 6x^2 - 4x - 1)\ln(x) + 9x - 1) + 72(x-1)(x+1)^2\mathrm{Li}_2(-x)(\ln(x) - 2\ln(x+1) + 1) + 84L_{\mu_F}x^2 + 12L_{\mu_F}x^2\ln^2(x) - 24L_{\mu_F}x^2\ln(x) - 180L_{\mu_F}x + 12L_{\mu_F}\ln^2(x) + 60L_{\mu_F}\ln(x) + 96L_{\mu_F} + 96x^3\mathrm{S}_{1,2}(1-x)$$

$$
\begin{aligned}
&- 144x^3\mathrm{S}_{1,2}(-x) + 300x^2\mathrm{S}_{1,2}(1-x) - 144x^2\mathrm{S}_{1,2}(-x) - 192x\mathrm{S}_{1,2}(1-x)\\
&+ 144x\mathrm{S}_{1,2}(-x) + 12\mathrm{S}_{1,2}(1-x) + 144\mathrm{S}_{1,2}(-x) - 24x^3\mathrm{Li}_3(-x) - 72x^2\mathrm{Li}_3(1-x)\\
&- 24x^2\mathrm{Li}_3(-x) + 24x\mathrm{Li}_3(-x) - 24\mathrm{Li}_3(1-x) + 24\mathrm{Li}_3(-x) + 36x^3\zeta_2\\
&+ 24x^3\zeta_2\ln(x) - 72x^3\zeta_2\ln(x+1) - 78x^3 + 4x^3\ln^3(x) - 90x^3\ln^2(x)\\
&- 72x^3\ln(x)\ln^2(x+1) + 60x^3\ln^2(x)\ln(x+1) + 72x^3\ln(x)\ln(x+1)\\
&+ 36x^2\zeta_2 + 24x^2\zeta_2\ln(x) - 72x^2\zeta_2\ln(x+1) - 240x^2 + 6x^2\ln^3(x)\\
&+ 24x^2\ln(1-x)\ln^2(x) + 54x^2\ln^2(x) - 72x^2\ln(x)\ln^2(x+1)\\
&+ 60x^2\ln^2(x)\ln(x+1) + 168x^2\ln(1-x) - 48x^2\ln(1-x)\ln(x)\\
&+ 42x^2\ln(x) + 72x^2\ln(x)\ln(x+1) - 36x\zeta_2 - 24x\zeta_2\ln(x) + 72x\zeta_2\ln(x+1)\\
&- 24\zeta_2\ln(x) + 72\zeta_2\ln(x+1) + 762x - 12x\ln^3(x) - 14\ln^3(x) + 84x\ln^2(x)\\
&+ 72x\ln(x)\ln^2(x+1) - 60x\ln^2(x)\ln(x+1) + 24\ln(1-x)\ln^2(x)\\
&- 93\ln^2(x) + 72\ln(x)\ln^2(x+1) - 60\ln^2(x)\ln(x+1) - 360x\ln(1-x)\\
&+ 162x\ln(x) - 72x\ln(x)\ln(x+1) + 192\ln(1-x) + 120\ln(1-x)\ln(x)\\
&-276\ln(x) - 72\ln(x)\ln(x+1) - 36\zeta_2 - 444).
\end{aligned}
\tag{B11}
$$

The singlet contributions for the (anti)quark-(anti)quark channel include terms arising from identical initial quarks, and nonidentical ones. These are given by the following expressions:

$$
\begin{aligned}
\Delta_{qq}^{(2)\mathrm{id}} = 2\Bigg(&L_{\mu_F}\Bigg(-\frac{1}{x+1}(4(x^2+1)(4\mathrm{Li}_2(-x) - \ln^2(x) + 4\ln(x+1)\ln(x) + 2\zeta_2))\\
&+8(x+1)\ln(x) - 16(x-1)\Bigg) - \frac{1}{3(x+1)}(4(x^2+1)(-18\mathrm{Li}_2(1-x)\ln(x)\\
&+ 12\mathrm{Li}_2(-x)(2\ln(1-x) - 2\ln(x) + \ln(x+1)) - 24\mathrm{Li}_3\left(\frac{1-x}{x+1}\right) + 24\mathrm{Li}_3\left(\frac{x-1}{x+1}\right)\\
&- 24\mathrm{S}_{1,2}(1-x) + 12\mathrm{S}_{1,2}(-x) + 24\mathrm{Li}_3(1-x) + 6\mathrm{Li}_3(-x) - 9\zeta_2\ln(x) + 12\zeta_2\ln(1-x)\\
&+ 6\zeta_2\ln(x+1) + 2\ln^3(x) - 6\ln(1-x)\ln^2(x) - 21\ln(x+1)\ln^2(x)\\
&+6\ln^2(x+1)\ln(x) + 24\ln(1-x)\ln(x+1)\ln(x) + 3\zeta_3)) + (1-x)\\
&\times(-16\mathrm{Li}_2(-x)\ln(x+1) - 16\mathrm{S}_{1,2}(-x) + 8\mathrm{Li}_3(-x) + 4\zeta_2\ln(x) - 8\zeta_2\ln(x+1)\\
&-\frac{2}{3}\ln^3(x) + 4\ln(x+1)\ln^2(x) - 8\ln^2(x+1)\ln(x) + 32\ln(1-x) + 8\zeta_3 - 34)\\
&+ 4(x+1)(2\mathrm{Li}_2(-x) + 4\ln(1-x)\ln(x) + 2\ln(x)\ln(x+1) + \zeta_2)\\
&+ 8(x+3)\mathrm{Li}_2(1-x) - 4(3x+1)\ln^2(x) + 2(7x-9)\ln(x)\Bigg) - \frac{4}{3}(x-1)^2\\
&\times(6\mathrm{Li}_2(1-x)(2\ln(x)+3) + 12\mathrm{S}_{1,2}(1-x) - 12\mathrm{Li}_3(1-x) + 2\ln^3(x) + 9\ln^2(x))\\
&+ 4(6x-7)\ln(x) - 26x^2 + 56x - 30
\end{aligned}
\tag{B12}
$$

$$
\begin{aligned}
\Delta_{qq}^{(2)\mathrm{non-id}} = \frac{1}{54x}(&36\mathrm{Li}_2(1-x)(x(12L_{\mu_F}(x+1) + x(8x+15) + 39) + 6x(x+1)\\
&\times(4\ln(1-x) + \ln(x)) + 16) + 6x\ln(x)(18L_{\mu_F}^2(x+1) + 36\ln(1-x)\\
&\times(2(L_{\mu_F}+3)x + 2L_{\mu_F} + 2(x+1)\ln(1-x) + 4x^2 + 3)\\
&+18L_{\mu_F}(4x^2+6x+3) + 20x^2 - 72(x+1)\zeta_2 - 48x + 345)
\end{aligned}
$$

$$
\begin{aligned}
&+(x-1)(-18L_{\mu_F}^2(x(4x+7)+4)+24\ln(1-x)\\
&\times(-3L_{\mu_F}(x(4x+7)+4)-3(x(4x+7)+4)\ln(1-x)+(17-22x)x-22)\\
&-12L_{\mu_F}(x(22x-17)+22)+703x^2+72(x(4x+7)+4)\zeta_2-1895x-116)\\
&-9x\ln^2(x)(24L_{\mu_F}(x+1)+48(x+1)\ln(1-x)+5(x(8x+15)+3))\\
&+432x(x+1)(3\mathrm{S}_{1,2}(1-x)-2\mathrm{Li}_3(1-x))+162x(x+1)\ln^3(x)).
\end{aligned}
\tag{B13}
$$

It is worth noticing the sign difference in the nonidentical vectorial contribution for the qq initial state, with respect to $q\bar{q}$:

$$
\begin{aligned}
\Delta_{q\bar{q}}^{(2)\text{non-id,V}} = -\Delta_{qq}^{\text{non-id,V}} = \frac{1}{3x}&(2(12\mathrm{Li}_2(-x)(2(2x^2+5)\ln(x)+5x(x+1)-6(x(x+2)+2)\\
&\times\ln(x+1))-6x\mathrm{Li}_2(1-x)(4x+(x-10)\ln(x)-5)+6(3x((x-2)\mathrm{Li}_3(1-x)\\
&-4(x+2)\mathrm{S}_{1,2}(-x))+4(x(x+2)+2)\mathrm{S}_{1,2}(1-x)+2(10-3x)x\mathrm{Li}_3(-x))\\
&-144\mathrm{S}_{1,2}(-x)+24\mathrm{Li}_3(1-x)-120\mathrm{Li}_3(-x)+30x(x(\zeta_2+4)+\zeta_2-4)\\
&+6\ln(x+1)(5\ln(x)(2x(x+1)+(x(x+2)+2)\ln(x))-6(x(x+2)+2)\zeta_2)\\
&-x\ln(x)(-6x\zeta_2+48x+x\ln(x)(4\ln(x)+39)-60\zeta_2+60)-18((x-6)x\\
&+4)\zeta_3-36(x(x+2)+2)\ln(x)\ln^2(x+1)))
\end{aligned}
\tag{B14}
$$

$$
\begin{aligned}
\Delta_{q\bar{q}}^{(2)\text{non-id,A}} = &\,4\mathrm{Li}_2(1-x)((3x+2)\ln(x)+1)+8\mathrm{Li}_2(-x)(x+8\ln(x)-6(x+2)\ln(x+1)+1)\\
&+4(4(x+2)\mathrm{S}_{1,2}(1-x)-x(12\mathrm{S}_{1,2}(-x)+\mathrm{Li}_3(1-x)-10\mathrm{Li}_3(-x)))\\
&-96\mathrm{S}_{1,2}(-x)+\frac{2}{3}(-72\mathrm{Li}_3(-x)+6(x(\zeta_2+9\zeta_3+4)+\zeta_2-6\zeta_3-4)\\
&+6\ln(x+1)(-6(x+2)\zeta_2+5(x+2)\ln^2(x)+2(x+1)\ln(x))\\
&+\ln(x)(6(5x\zeta_2+2\zeta_2-2)-x\ln(x)(4\ln(x)+3))\\
&-36(x+2)\ln(x)\ln^2(x+1))+8\mathrm{Li}_3(1-x).
\end{aligned}
\tag{B15}
$$

The correction terms that appear in the qg and $q\gamma$ channels are given by the following expressions:

$$
\begin{aligned}
\Delta_{qg}^{(2)C_A} = \frac{1}{2}&\left(\frac{2}{9}L_{\mu_F}(36(2x^2+6x+3)\mathrm{Li}_2(1-x)-36(2x^2+2x+1)(\mathrm{Li}_2(-x)\right.\\
&+\ln(x)\ln(x+1))-72(2x^2-x+1)\zeta_2+73x^2+54(2x^2-2x+1)\ln^2(1-x)\\
&+6\left(-71x^2+54x+\frac{8}{x}+9\right)\ln(1-x)+18(28x^2-2x+3)\ln(x)\\
&+36(-2x^2+10x+1)\ln(1-x)\ln(x)-12x+\frac{44}{x}-36(3x+1)\ln^2(x)-87)\\
&-4(2x^2+2x+1)(4\mathrm{Li}_2(-x)(\ln(1-x)-\ln(x))+2\mathrm{Li}_3(-x)-4\mathrm{Li}_3\left(\frac{1-x}{x+1}\right)\\
&+4\mathrm{Li}_3\left(\frac{x-1}{x+1}\right)-3\ln(x+1)\ln^2(x)+4\ln(1-x)\ln(x+1)\ln(x))\\
&+\frac{4}{3}\left(44x^2+90x+\frac{16}{x}+33\right)\mathrm{Li}_2(1-x)+8(5x^2+10x+7)\mathrm{Li}_2(1-x)\ln(1-x)\\
&+8(4x^2+5x+1)(\mathrm{Li}_2(-x)+\ln(x)\ln(x+1))+8x\mathrm{Li}_2(1-x)\\
&+8x(7-2x)\mathrm{Li}_2(1-x)\ln(x)+\frac{2}{3}L_{\mu_F}^2\left(-31x^2+6(2x^2-2x+1)\ln(1-x)+24x\right.\\
&\left.\left.+\frac{4}{x}+6(4x+1)\ln(x)+3\right)+8(4x^2+16x+9)\mathrm{S}_{1,2}(1-x)-4(12x^2+34x+15)\mathrm{Li}_3(1-x)\right.
\end{aligned}
$$

$$
\begin{aligned}
&+\frac{4}{3}\left(107x^2-84x-\frac{8}{x}+15\right)\zeta_2-32(2x^2-x+1)\zeta_2\ln(1-x)\\
&-4(2x^2+4x+1)\zeta_3+\frac{1837x^2}{27}+\frac{26}{3}(2x^2-2x+1)\ln^3(1-x)\\
&+\frac{4}{3}\left(-77x^2+63x+\frac{8}{x}+6\right)\ln^2(1-x)+4(-6x^2+22x+1)\ln(x)\ln^2(1-x)\\
&+4(2x^2-14x-3)\ln^2(x)\ln(1-x)-\left(\frac{346x^2}{3}+5\right)\ln^2(x)+\frac{2}{9}\left(74x^2+75x+\frac{88}{x}-210\right)\\
&\times\ln(1-x)+20(13x^2-2x+1)\ln(x)\ln(1-x)-\frac{2}{9}(457x^2+12x\\
&-354)\ln(x)+16x(2x-5)\zeta_2\ln(x)-\frac{1226x}{9}+\frac{116}{27x}+\frac{2}{3}(20x+9)\ln^3(x)\\
&-4x\ln^2(x)+8x\ln(x)\ln(1-x)-8x\ln(x)+\frac{539}{9}\Bigg)
\end{aligned}
\tag{B16}
$$

$$
\begin{aligned}
\Delta_{qg}^{(2)C_F}=\frac{1}{2}\Bigg(&L_{\mu_F}(-48x^2\mathrm{Li}_2(1-x)+(2x^2-2x+1)(36\ln^2(1-x)-8\zeta_2)+22x^2\\
&+8(4x^2-2x+1)\ln^2(x)-4(23x^2-34x+8)\ln(1-x)+2(46x^2-40x+5)\\
&\times\ln(x)-8(16x^2-10x+5)\ln(1-x)\ln(x)-68x+24)+(2x^2-2x+1)\\
&\left(-16\mathrm{Li}_2(-x)\ln(x)+32\mathrm{Li}_3(-x)-16\zeta_2\ln(1-x)+\frac{70}{3}\ln^3(1-x)+100\zeta_3\right)\\
&+2(40x^2-28x+3)\mathrm{Li}_2(1-x)-4(26x^2-6x+3)\mathrm{Li}_2(1-x)\ln(1-x)\\
&-16(3x^2+2x-1)(\mathrm{Li}_2(-x)+\ln(x)\ln(x+1))+8(x-3)\mathrm{Li}_2(1-x)+4(1-2x)\\
&\times\mathrm{Li}_2(1-x)\ln(x)+3L_{\mu_F}^2((8x^2-8x+4)\ln(1-x)+(-8x^2+4x-2)\\
&\times\ln(x)+4x-1)-4(34x^2-22x+11)\mathrm{S}_{1,2}(1-x)+4(18x^2+2x-1)\mathrm{Li}_3(1-x)\\
&+4(-12x^2+2x+5)\zeta_2+24(4x^2-2x+1)\zeta_2\ln(x)-\frac{305x^2}{2}-\frac{1}{3}(52x^2-34x+17)\ln^3(x)\\
&-\frac{1}{2}(4x^2-68x+35)\ln^2(x)+8(10x^2-6x+3)\ln(1-x)\ln^2(x)\\
&-6(22x^2-14x+7)\ln^2(1-x)\ln(x)-2(63x^2-80x+23)\ln^2(1-x)-(174x^2\\
&-245x+59)\ln(x)+4(48x^2-50x+13)\ln(1-x)\ln(x)+2(88x^2-147x+38)\\
&\times\ln(1-x)-12(x-1)+233x-4(x-3)\ln^2(x)+(28-44x)\ln(x)+8(x-3)\\
&\times\ln(1-x)\ln(x)+24(x-1)\ln(1-x)-\frac{181}{2}\Bigg).
\end{aligned}
\tag{B17}
$$

The last correction terms correspond to the ones contributing to the gg, $g\gamma$ and $\gamma\gamma$ channels:

$$
\begin{aligned}
\Delta_{gg}^{(2)C_A}=&\frac{C_A^2}{C_A^2-1}\frac{1}{3}(-8(x+1)^2\mathrm{Li}_2(-x)(9\ln(x)-6\ln(x+1)-2)-24(x-1)^2\mathrm{S}_{1,2}(1-x)\\
&+48(x+1)^2\mathrm{S}_{1,2}(-x)+72x(x+2)\mathrm{Li}_3(-x)+72\mathrm{Li}_3(-x)+x(x(8\zeta_2+48\zeta_3+191)\\
&+16(\zeta_2+6\zeta_3-9))+24\zeta_2\ln(x+1)+4\ln(x+1)(6x(x+2)\zeta_2+(x+1)^2(4-9\ln(x))\ln(x))\\
&+24(x+1)^2\ln(x)\ln^2(x+1)+2\ln(x)(-x(75x+38)+(x(25x+2)-2)\\
&\times\ln(x)-6)+8\zeta_2+48\zeta_3-47)
\end{aligned}
\tag{B18}
$$

$$
\begin{aligned}
\Delta_{qg}^{(2)C_F} = {} & L_{\mu_F}((2x+1)^2(2\ln(x)(\ln(x)-4\ln(1-x))-8\mathrm{Li}_2(1-x))-67x^2+60x \\
& +16(x-1)(3x+1)\ln(1-x)+2(1-4(x-2)x)\ln(x)+7)-4(x+1)^2 \\
& \times(\ln(x+1)(4\mathrm{Li}_2(-x)-3\ln^2(x)+2\ln(x+1)\ln(x)+2\zeta_2)+4\mathrm{S}_{1,2}(-x)) \\
& -4(2x+1)^2(\mathrm{Li}_2(1-x)(4\ln(1-x)+\ln(x))-4\mathrm{Li}_3(1-x)+\ln(1-x) \\
& \times(2\ln(1-x)-\ln(x))\ln(x))+4(2x(7x-2)-5)\mathrm{Li}_2(1-x)+8(x(x+4)+2) \\
& \times\mathrm{Li}_2(-x)\ln(x)+8(x+1)(\mathrm{Li}_2(-x)+\ln(x)\ln(x+1))-2L_{\mu_F}^2 \\
& \times(-6x^2+4x+(2x+1)^2\ln(x)+2)-8(x(7x+10)+1)\mathrm{S}_{1,2}(1-x)+8((x-2)x-1) \\
& \times\mathrm{Li}_3(-x)+98x^2+4(3(3-4x)x+5)\zeta_2+4(10x(x+1)+3)\zeta_2\ln(x)+4(2(x-1)x-1)\zeta_3 \\
& -66x-\frac{2}{3}(8x(x+1)+3)\ln^3(x)-2(x+1)(4x+3)\ln^2(x)+16(x-1) \\
& \times(3x+1)\ln^2(1-x)+(x(105x-64)-23)\ln(x)+4(1-4(x-2)x)\ln(1-x) \\
& \times\ln(x)-2(x-1)(67x+7)\ln(1-x)-32. \qquad \text{(B19)}
\end{aligned}
$$

[1] S. Dittmaier, A. Huss, and C. Speckner, J. High Energy Phys. 11 (2012) 095.
[2] S. Dittmaier, A. Huss, and C. Speckner, Proc. Sci. DIS2013 (**2013**) 283 [arXiv:1306.6298].
[3] R. D. Ball *et al.* (NNPDF Collaboration), J. High Energy Phys. 04 (2015) 040.
[4] L. A. Harland-Lang, A. D. Martin, P. Motylinski, and R. S. Thorne, Eur. Phys. J. C **75**, 204 (2015).
[5] S. Dulat, T.-J. Hou, J. Gao, M. Guzzi, J. Huston, P. Nadolsky, J. Pumplin, C. Schmidt, D. Stump, and C. P. Yuan, Phys. Rev. D **93**, 033006 (2016).
[6] M. L. Mangano, Adv. Ser. Dir. High Energy Phys. **26**, 231 (2016).
[7] D. de Florian, G. F. R. Sborlini, and G. Rodrigo, Eur. Phys. J. C **76**, 282 (2016).
[8] D. de Florian, G. F. R. Sborlini, and G. Rodrigo, J. High Energy Phys. 10 (2016) 056.
[9] A. Manohar, P. Nason, G. P. Salam, and G. Zanderighi, Phys. Rev. Lett. **117**, 242002 (2016).
[10] A. V. Manohar, P. Nason, G. P. Salam, and G. Zanderighi, J. High Energy Phys. 12 (2017) 046.
[11] G. Altarelli, R. K. Ellis, and G. Martinelli, Nucl. Phys. **B157**, 461 (1979).
[12] R. Hamberg, W. L. van Neerven, and T. Matsuura, Nucl. Phys. **B359**, 343 (1991); **B644**, 403(E) (2002).
[13] W. L. van Neerven and E. B. Zijlstra, Nucl. Phys. **B382**, 11 (1992); **B680**, 513(E) (2004).
[14] R. V. Harlander and W. B. Kilgore, Phys. Rev. Lett. **88**, 201801 (2002).
[15] S. Catani, L. Cieri, G. Ferrera, D. de Florian, and M. Grazzini, Phys. Rev. Lett. **103**, 082001 (2009).
[16] K. Melnikov and F. Petriello, Phys. Rev. Lett. **96**, 231803 (2006).
[17] K. Melnikov and F. Petriello, Phys. Rev. D **74**, 114017 (2006).
[18] R. Gavin, Y. Li, F. Petriello, and S. Quackenbush, Comput. Phys. Commun. **182**, 2388 (2011).
[19] R. Gavin, Y. Li, F. Petriello, and S. Quackenbush, Comput. Phys. Commun. **184**, 208 (2013).
[20] R. Boughezal, J. M. Campbell, R. K. Ellis, C. Focke, W. Giele, X. Liu, F. Petriello, and C. Williams, Eur. Phys. J. C **77**, 7 (2017).
[21] T. Ahmed, M. Mahakhud, N. Rana, and V. Ravindran, Phys. Rev. Lett. **113**, 112002 (2014).
[22] S. Catani, L. Cieri, D. de Florian, G. Ferrera, and M. Grazzini, Nucl. Phys. **B888**, 75 (2014).
[23] S. Dittmaier and M. Krämer, Phys. Rev. D **65**, 073007 (2002).
[24] U. Baur and D. Wackeroth, Phys. Rev. D **70**, 073015 (2004).
[25] C. M. Carloni Calame, G. Montagna, O. Nicrosini, and A. Vicini, J. High Energy Phys. 12 (2006) 016.
[26] U. Baur, O. Brein, W. Hollik, C. Schappacher, and D. Wackeroth, Phys. Rev. D **65**, 033007 (2002).
[27] U. Baur, S. Keller, and W. K. Sakumoto, Phys. Rev. D **57**, 199 (1998).
[28] S. Actis, A. Ferroglia, M. Passera, and G. Passarino, Nucl. Phys. **B777**, 1 (2007).
[29] S. Actis and G. Passarino, Nucl. Phys. **B777**, 35 (2007).
[30] S. Actis and G. Passarino, Nucl. Phys. **B777**, 100 (2007).
[31] G. Degrassi and A. Vicini, Phys. Rev. D **69**, 073007 (2004).
[32] Q.-H. Cao and C. P. Yuan,Phys. Rev. Lett. **93**, 042001 (2004).
[33] G. Balossini, G. Montagna, C. M. Carloni Calame, M. Moretti, O. Nicrosini, F. Piccinini, M. Treccani, and A. Vicini, J. High Energy Phys. 01 (2010) 013.
[34] N. E. Adam, V. Halyo, S. A. Yost, and W. Zhu, J. High Energy Phys. 09 (2008) 133.
[35] Y. Li and F. Petriello, Phys. Rev. D **86**, 094034 (2012).
[36] L. Barze, G. Montagna, P. Nason, O. Nicrosini, F. Piccinini, and A. Vicini, Eur. Phys. J. C **73**, 2474 (2013).

[37] S. Dittmaier, A. Huss, and C. Schwinn, Proc. Sci. LL2014 (**2014**) 045 [arXiv:1405.6897].
[38] S. Dittmaier, A. Huss, and C. Schwinn, Nucl. Phys. **B885**, 318 (2014).
[39] S. Dittmaier, A. Huss, and C. Schwinn, Nucl. Phys. **B904**, 216 (2016).
[40] S. Catani and M. Grazzini, Phys. Rev. Lett. **98**, 222002 (2007).
[41] R. Bonciani, F. Buccioni, R. Mondini, and A. Vicini, Eur. Phys. J. C **77**, 187 (2017).
[42] R. Bonciani, S. Di Vita, P. Mastrolia, and U. Schubert, J. High Energy Phys. 09 (2016) 091.
[43] A. Buckley, J. Ferrando, S. Lloyd, K. Nordström, B. Page, M. Rüfenacht, M. Schönherr, and G. Watt, Eur. Phys. J. C **75**, 132 (2015).
[44] J. Butterworth *et al.*, J. Phys. G **43**, 023001 (2016).